Bull. ERS, No.11 (1977)

PREDICTION OF ACCELERATION RESPONSE SPECTRA FOR GIVEN EARTHQUAKE MAGNITUDE, EPICENTRAL DISTANCE AND SITE CONDITIONS

By

Tsuneo KATAYAMA,[I] Toshio IWASAKI[II] and Mitsuaki SAEKI[III]

SYNOPSIS

Statistical analysis was made for 277 acceleration response spectral amplitudes at each of the 18 natural periods of a SDOF system in terms of earthquake magnitude, epicentral distance and recording-site conditions. The accelerograms used for analysis were those recorded during 19 years from 1956 to 1974 by strong-motion accelerographs installed on the ground surface at various locations in Japan.

An empirical formula was obtained from the results of the statistical analysis to predict the acceleration spectral amplitude $\overline{SA}$ (h=0.05) for a given period of a SDOF system for a given set of M, Δ and site conditions as a simple product of three factors. The quantitative characteristics of the effects of these parameters on acceleration response spectra were discussed. From the analysis of the distribution of the 277 ratios of observed amplitudes SA to predicted amplitudes $\overline{SA}$ at each natural period, empirical factors were obtained that produce the acceleration response amplitudes for given probabilities of being exceeded.

INTRODUCTION

The response spectrum technique is widely used for the dynamic analysis of structures subjected to seismic excitations. The response spectrum of an actual earthquake record exhibits two principal features, i.e. the frequency characteristics and the severity of shaking of the ground motion. The former is characterized by the shape of spectrum, whereas the latter by the spectral amplitude. A design response spectrum is obtained from a number of spectra computed from actual recorded strong earthquake

---

I) Institute of Industrial Science, University of Tokyo.

II) Ground Vibration Section, Earthquake Disaster Prevention Division, Public Works Research Institute, Ministry of Construction.

III) Japan Engineering Consultants Co., Ltd.

motions usually through normalization and averaging. Normalization is performed to each spectrum in order to extract the frequency characteristics alone. This enables one to compare the shapes of spectra calculated from different accelerograms in terms of the same scale. In Japan, acceleration response spectra are commonly normalized by the peak acceleration of the record. Normalized response spectra are often classified into several groups according to recording-site ground conditions. They are then averaged and smoothed to obtain design acceleration magnification spectra. A typical example of such spectra is shown in Figure 1 which was proposed by the Public Works Research Institute[1] (Ministry of Construction, Japan).

Although such a design spectrum is doubtlessly an efficient and practical engineering tool for the earthquake-resistant design of structures, it should be pointed out that some of the important characteristics contained in each original response spectrum are lost through the process of normalization and averaging. It is well recognized, at least qualitatively, that spectral shape is influenced by earthquake magnitude and source-to-site distance. However, most of the conventional design spectra do not explicitly take account of these effects.

For the earthquake-resistant analysis of very important installations in recent years, the occurrences of probable hypothetical earthquakes are often assumed in the area surrounding the site under consideration by taking into account the seismic and geological environment of the area. In order to evaluate the characteristics of ground motions caused by these earthquakes, it is important to consider the effects of magnitude and distance on spectral shape.

Problems similar to the one to be discussed in this paper have been treated by previous investigators. McGuire[2] studied the distribution of response of a SDOF linear oscillator to 68 horizontal components of accelerograms obtained at 21 sites in the U.S. during 22 earthquakes. Pseudo-velocity response spectral amplitudes at each of 16 natural frequencies were regressed for each of four values of damping (0, 2, 5 and 10% of critical) in terms of earthquake magnitude and hypocentral distance. No record was used for which significant soil amplification of the motion has been established. Other than this, no distinction was made between records from rock sites and those from alluvial sites. Trifunac[3] presented an empirical model for scaling Fourier amplitude spectra of strong earthquake ground acceleration in terms of magnitude, epicentral distance and recording-site conditions. Trifunac[4] recently applied the same methodology for scaling absolute acceleration response spectra. His empirical equation for forecasting acceleration spectra involves earthquake magnitude, epicentral distance, recording-site conditions, ground-motion component direction and the desired confidence level. The form of the equation looks complicated and the inevitableness of taking that particular functional form does not seem very clear.

The results of statistical analysis of absolute acceleration response spectra of 277 horizontal components of earthquake ground motions recorded in Japan are reported in this paper. The method of statistical analysis adopted here is different from those used by previous investigators. Earthquake magnitude, epicentral distance and site ground conditions were chosen as three principal parameters. No functional relationship was assumed between the spectral amplitude and these parameters. Prediction of an average acceleration spectral amplitude may be performed by simply calculating a product of three factors, and the average spectrum may be modified to obtain the spectrum with a specified probability of being exceeded through an additional multiplication.

DATA BASE

As of January 31, 1977, there are 1,096 strong-motion accelrographs installed in Japan according to the catalogue prepared by the Strong-Motion Observation Council in the National Research Center for Disaster Prevention (Science and Technology Agency, Japan). About two-thirds of these accelerographs are installed at structures such as buildings, bridges, dams and other civil engineering structures. In the present study, only "free-field" accelrograms recorded at stations on the ground surface were used. Figure 2 shows the frequency characteristics of the most typical accelrograph (SMAC-B2 Type) used in the Japanese strong-motion earthquake measurement network. Since no correction was made with respect to the frequency characteristics of accelerograph, it should be noted that higher frequency components of a record are considerably suppressed.

A total of 277 horizontal components of accelrograms recorded in 19 years between 1956 and 1974 during 67 earthquakes were used for analysis. Of the 277 component records, 182 were obtained by the network maintained by the Public Works Research Institute (Ministry of Construction), 78 by the Port and Harbour Research Institute (Ministry of Transport) and the rest by other organizations. Figure 3 shows the distribution of magnitudes for the 67 earthquakes. Earthquakes with magnitude less than 4.5 or with focal depth greater than 60 km were not included in the data. About three-quarters of the earthquakes have magnitudes between 5 and 7. Only four earthquakes with magnitude greater than 7.5 were used, which include the 1964 Niigata and the 1968 Tokachi-oki earthquake. The largest number of components in the data recorded during a single earthquake was 14, which were obtained during the 1968 Tokachi-oki earthquake. Figure 4 shows the distribution of peak accelerations of the 277 records. It is seen that about 80% of the data correspond to accelerograms with peak acceleration less than 100 cm/sec^2.

The absolute acceleration response spectrum curve was represented by spectral amplitudes at 18 discrete natural periods as follows:

$$T = 0.1,\ 0.15,\ 0.2,\ 0.25,\ 0.3,\ 0.35,\ 0.4,\ 0.5,\ 0.6,\ 0.7,\ 0.8,\ 0.9,\ 1.0,\ 1.5,\ 2.0,\ 2.5,\ 3.0,\ \text{and } 4.0\ \text{(sec)} \qquad (1)$$

The damping of the SDOF system was assumed to be 5% of critical. It was considered that spectral values required for most engineering purposes may be reasonably well estimated if a 5%-damped spectrum is available. The spectral values of the 78 components of accelerograms recorded by the Port and Harbour Research Institute network were extracted from published reports.[5,6,7]

METHOD OF ANALYSIS

Assume a set of N observed values and let the i-th value be denoted by A_i. Select R items that are likely to have contributed to realizing the sample value A_i. Each item is then divided into several categories.

Define a variable x_{ijk} corresponding to category k in item j of sample i so that this variable takes a value of 1 (one) if the properties of sample i react to category k in item j, and 0 (zero) otherwise. (Strictly speaking, k should carry suffix j as k_j, but j is dropped for simplicity.) Denote the unknown category value for category k in item j by w_{jk} and consider a quantity

$$\alpha_i = \sum_{j=1}^{R} \sum_{k=1}^{K_j} x_{ijk} w_{jk} \qquad (2)$$

in which K_j is the number of categories in item j. The number of unknown category values is given by

$$\sum_{j=1}^{R} K_j \qquad (3)$$

and w_{jk}'s are determined in such a way that the N observed values A_i best agree with the N predicted values α_i. The criterion used for the best agreement is to minimize the sum of the squares of the differences between observed and predicted values:

$$\sum_{i=1}^{N} (A_i - \alpha_i)^2 \rightarrow \text{Minimum} \qquad (4)$$

Once the optimum w_{jk}'s are determined, the correlation coefficient

$$\rho = \frac{(1/N)\Sigma A_i \alpha_i - \bar{A}\,\bar{\alpha}}{\sigma_A \sigma_\alpha} \tag{5}$$

indicates whether or not the actual phenomenon is satisfactorily described by the statistical model. In equation (5), $\bar{A}$ and $\bar{\alpha}$ are the means, and σ_A and σ_α are the standard deviations of A_i and α_i, respectively. The statistical method discussed here is often called "Type I Quantification Analysis" in Japan[8].

It is seen that equation (2) assumes that a predicted value is obtained by the sum of relevant category values. If it is considered appropriate to assume that a predicted value be obtained by the product of category values, equation (2) should be replaced by

$$\alpha_i = \prod_{j=1}^{R} \prod_{k=1}^{K_j} w_{jk}^{x_{ijk}} \tag{6}$$

By taking the logarithms of the both sides of equation (8), the mathematical expression is reduced to

$$\log \alpha_i = \sum_{j=1}^{R} \sum_{k=1}^{K_j} x_{ijk}(\log w_{jk}) \tag{7}$$

which is essentially the same in form as equation (2). Now, the quantities $\bar{A}$, $\bar{\alpha}$, σ_A and σ_α in equation (5) are the means and the standard deviations of $\log A_i$ and $\log \alpha_i$, respectively.

APPLICATION TO SPECTRAL AMPLITUDE DATA

Statistical analysis was performed for the 277 acceleration spectral amplitudes (h=5% of critical) at the 18 natural periods shown in equation (1) by using the method described in the preceding section. Three items in the present analysis are earthquake magnitude, epicentral distance and ground conditions of recording-site. Shortcomings associated with selecting only three parameters are well acknowledged, but they are not discussed here. The main purpose of the study was to obtain useful information from the practical earthquake engineering point of view. Refinement of analysis is only achieved at the expense of a significant number of data points. This is the main reason for simply choosing epicentral distance as the measure of source-to-site distance and for using crude but code-oriented classifications of ground conditions.[9]

The items and categories used in the present study are listed in Table 1. It is noted that magnitude and epicentral distance, which are continuous quantities in nature, are also divided into several discrete categories. By using these categories in the method previously mentioned, no functional relationship need be assumed between the spectral amplitude and the relevant parameters.

Table 2 shows the distribution of the number of data points in each of the combinations of items and categories. As may be seen from this table, the data used in this study are far from sufficient in number nor uniform in distribution. The quality of data set may be improved only when more records become available. The results of the present analysis should be carefully treated and interpreted by taking into account the inherent characteristics of the data set.

After examining the results of the preliminary analysis[10] which assumed the additive prediction formula, equation (2), it was considered that the multiplicative formula, equation (6), is preferable because of the physical structure of the phenomenon under consideration. In addition, a predicted spectral amplitude is always positive for the multiplicative formula.

The prediction formula, therefore, takes the following form:

$$\overline{SA}(T,h) = f_M(T,h)*f_\Delta(T,h)*f_{GC}(T,h) \qquad (8)$$

where

$\overline{SA}(T,h)$ = Predicted absolute acceleration response spectral amplitude for given T and h,

T = Natural period of SDOF system (sec),

h = 0.05 = Damping factor of SDOF system,

$f_M(T,h)$ = Weighting factor for each magnitude category in Table 1,

$f_\Delta(T,h)$ = Weighting factor for each distance category in Table 1, and

$f_{GC}(T,h)$ = Weighting factor for each ground condition category in Table 1.

The values of weighting factors determined from the statistical analysis are shown in Table 3 for each of the 18 periods specified in equation (1). For example, the absolute acceleration response spectral amplitude for T=0.5 sec and h=0.05 that would be obtained from the ground motions caused by an earthquake with M=6.1-6.7 and Δ=20-59 km, and recorded on Type III ground is predicted by equation (8) and Table 3 as follows:

$$\overline{SA}(0.5,\ 0.05) = 0.309 \times 2.91 \times 140 = 126\ (\mathrm{cm/sec}^2)$$

Several predicted response spectra are shown in Figure 5.

Since Table 3 gives the raw outputs from the statistical analysis, the spectra that would be computed from equation (8) are generally not smooth in shape. It should be also pointed out that several weighting factors in Table 3 are even contradictory as typically seen in the f_Δ-values for periods longer than 2.0 sec because no functional relation was assumed for the spectral amplitude in terms of the three parameter used in this analysis.

The second column in Table 3 shows correlation coefficients between observed and predicted spectral amplitudes for each natural period. Correlation is rather low especially for short periods. This indicates that not only the average predicted value $\overline{SA}$ but also the deviations of observed values about the predicted value should be carefully investigated. This problem will be discussed in one of the latter sections.

CHARACTERISTICS OF PREDICTED SPECTRA

Figure 6 shows the influence of earthquake magnitude on the absolute acceleration spectral amplitude for a fixed combination of distance and site condition categories. The effect is illustrated in terms of the ratio of the weighting factor of a certain magnitude category to that of the magnitude category between M=4.5 and M=5.3. It is seen that the effect of magnitude is different for different period ranges of a SDOF system. The increase of magnitude from the smallest (M=4.5-5.3) to the largest category (M=7.5-7.9) investigated in this study causes approximately 5 to 6-fold increase in the response acceleration for natural periods shorter than about 0.4 sec, whereas the same increase in magnitude produces approximately 14 to 20-fold increase in the response acceleration for periods longer than about 0.7 sec. This clearly indicates that large earthquakes are typically characterized by relatively greater content of long-period (i.e. low-frequency) waves, a trend repeatedly discussed by previous investigators. As far as Figure 6 is concerned, the effect of magnitude is most noticeable in the range of natural period between about 0.7 and 1.5 sec.

The effect of epicentral distance on the acceleration response spectrum is illustrated in Figure 7, in which are shown the ratios of weighting factors for different distance categories to that for Δ=200-405 km category. Generally speaking, the increase in response acceleration due to the decrease in epicentral distance is seen to be more pronounced for SDOF systems having natural periods shorter than about 0.8 sec. This substantiates the wellknown tendency that the ground motions caused by near earthquakes more strongly contain shorter-period component waves than those caused by far earthquakes.

Figure 8 shows the effect of recording-site ground conditions on the response spectra in terms of the ratios of weighting factors for different ground condition categories to that for Type I ground. It is interesting to note that, in spite of the crude and code-oriented classifications used for describing ground conditions, the effect of site conditions is very clearly demonstrated by the results of the present analysis. The effect is most noticeable in the period range of SDOF systems between 0.5 and 2.0 sec, in which the absolute acceleration response spectral amplitude increases as the soil becomes softer. For the period of structures shorter than about 0.3 sec, the spectral amplitude is relatively less affected by the type of the ground of recording-site, but is somewhat greater for the harder ground than for the softer ground.

SCATTER OF OBSERVED RESPONSES ABOUT PREDICTED RESPONSE

As is seen in the values of correlation coefficients in Table 3, correlation between predicted values $\overline{SA}$ and observed values SA cannot be regarded very high. This indicates that, although equation (8) gives a single predicted spectrum for a certain combination of magnitude, distance and ground conditions, observed spectra computed from accelerograms obtained for the same combination of categories do exhibit considerable deviations from the predicted spectrum. For example, according to Table 2 there are 32 component accelerograms recorded for the combination of M=6.1-6.7, Δ=20-59 km and Type III ground. Figure 9 shows the predicted spectrum for this particular combination of categories and the ranges of observed spectral amplitudes of the 32 accelerograms. There seem to be two principal reasons for such a wide scatter as shown in Figure 9 to be observed: (1) The numbers of catogories in each item are small. Each magnitude and distance category includes a wide range of variation, and the ground condition categories are not very specific. (2) Only three principal factors are selected that may influence spectral response amplitudes, but there are numerous other parameters which cannot be considered explicitly in the present analysis.

Let the ratio of an observed spectral amplitude SA and the predicted amplitude $\overline{SA}$ be denoted by α:

$$\alpha = SA/\overline{SA} \qquad (9)$$

There are 277 α-values available at each of the 18 periods given in equation (1). Figures 10 to 13 show the histograms of these ratios at four selected periods of a SDOF system. All of these histograms have distributions considerably skewed to the right and apparently resemble the lognormal distribution. The means and standard deviations of α are listed in columns(2) and (3) of Table

4. The χ^2 goodness-of-fit test was applied to the values of α by assuming the lognormal distribution with the parameters m_α and σ_α estimated from the data. The computed χ^2-values are shown in column (4) of Table 4 for the 18 periods investigated. Since the number of intervals used for this analysis was 15, the number of degree of freedom becomes 12 and the critical value at the 5% significance level is $\chi^2_{0.05,12} = 21.03$. Except for the two cases at T=0.15 and 0.2 sec in which the computed χ^2-values slightly exceed the critical value, all the other values are seen to be less than the critical. Therefore, it may be concluded that the data are not in significant contradiction to the lognormal model.

If α is assumed to be lognormally distributed, the value of α for a specified probability of being exceeded, p, can be easily evaluted. Such values of α for p=0.05, 0.1, 0.2, 0.3, 0.4 and 0.5 are given in Table 4. It is found that the values of α for a given probability p are almost constant regardless of period T. Hence the averages shown in the bottom line of Table 4 may be regarded as the representative values. When the predicted spectrum amplitude $\overline{SA}$ computed by equation (8) and Table 3 is combined with the factors given in Table 4, an absolute acceleration response spectrum for a given probability of being exceeded may be constructed.

CONCLUSIONS

The principal results of this study may be summarized as follows:

1. An empirical formula was obtained for predicting the spectral amplitude of absolute response acceleration of a SDOF system (h=0.05) for a given period and a given set of earthquake magnitude, epicentral distance and site conditions as a simple product of three weighting factors.

2. The effects of earthquake magnitude, distance and site conditions on the acceleration response spectrum were discussed in quantitative terms. The characteristics found from the study were in accordance with those qualitatively discussed by a number of previous investigators.

3. The effect of earthquake magnitude was found most noticeable in the period range longer than about 0.7 sec, in which the increase in spectral amplitude due to the increase in magnitude is more notable than in shorter-period range. The increase in spectral amplitude due to the decrease in epicentral distance is most pronouncedly found in the shorter-period range less than about 0.8 sec. The effect of site ground conditions is well demonstrated in the period range between 0.5 and 2.0 sec, in which the spectral amplitude generally increases as the soil becomes softer.

4. By using the fact that the ratio of observed and predicted amplitude, $\alpha=SA/\overline{SA}$, was found to be lognormally distributed, basic information was supplied that can be used to obtain the acceleration

response spectrum for a given probability of being exceeded.

In applying the results obtained from this study to predict response spectra, it is necessary to make engineering judgement especially by noting the following:

1. The data used for analysis are far from sufficient in number nor uniform in distribution. There is a serious shortage of accelerograms of large earthquakes, especially recorded at short epicentral distances.

2. Magnitude and distance categories have relatively wide ranges and the classifications of ground conditions involve considerable ambiguity.

ACKNOWLEDGEMENTS

The studies reported herein were made as a part of the comprehensive research project carried out by the Aseismic Technology Development Committee chaired by Dr. Shunzo Okamoto. The committee was established within the Technology Center for National Land Development under contract with the Public Works Research Institute (Ministry of Construction). The subcommittee on ground motion and soil problems was chaired by Dr. Keizaburo Kubo. In addition to recording their gratitude for the efforts of many individual members of the committee, the authors express special appreciation to Mr. Ken-ichi Tokida (Research Engineer, Ground and Vibration Section, Earthquake Disaster Prevention Division, Public Works Research Institute) and Mr. Hiroshi Shimamura (formerly, Structural Engineer, Japan Engineering Consultants Co., Ltd.) for assistance in preparing earthquake response spectra and in performing necessary computer processing of the data.

REFERENCES

1. E. Kuribayashi, T. Iwasaki, Y. Iida and K. Tuji, "Effects of seismic and subsoil conditions on earthquake response spectra", Proceedings of International Conference on Microzonation for Safer Construction Research and Application, 499-512 (1972).
2. R.K. McGuire, "Seismic structural risk analysis, incorporating peak response regressions on earthquake magnitude and distance", Structures Publications No. 399, R74-51, Dept. of Civil Eng., Massachusetts Institute of Technology (1974).
3. M.D. Trifunac, "Preliminary empirical model for scaling Fourier amplitude spectra for strong ground acceleration in terms of earthquake magnitude, source-to-station distance, and recording site conditions", Bull. Seism. Soc. Am., 66, 1343-1373 (1976).
4. M.D. Trifunac, "Forecasting the spectral amplitudes of strong earthquake ground motion", a paper presented at Panel Discussion 4 "Earthquake Parameters for Design of Major Projects",

Preprint of 6th World Conf. on Earthquake Eng., New Delhi (1977).

5. H. Tsuchida, T. Yamada, E. Kurata and K. Sudo, "Annual report on strong-motion earthquake records in Japanese ports (1963 and 1964)", Technical Note of Port and Harbour Research Institute, 55 (1968); "ditto (1965 and 1966)", ditto, 62 (1968).
6. H. Tsuchida, E. Kurata and K. Sudo, "ditto (1967)", ditto, 64 (1969); "Strong-motion earthquake records of the 1968 Tokachi-oki earthquake and its aftershocks", ditto, 80 (1969); "ditto (1968)", ditto, 98 (1970); "ditto (1969)", ditto 100 (1970); "ditto (1970)", ditto, 116 (1971).
7. E. Kurata, T. Ishizaka and H. Tsuchida, "ditto (1971)", ditto, 136 (1972); "ditto (1972)", ditto, 160 (1973); "ditto (1973)", ditto, 181 (1974); "ditto (1974)", ditto, 202 (1975).
8. C. Hayashi, "Sample survey and theory of quantification", Bull. Intern. Statistical Inst., 38, Part IV, 505-513, Tokyo (1961).
9. "Specifications for earthquake-resistant design of highway bridges", Japan Road Association (1971).
10. T. Iwasaki and T. Katayama, "Statistical analysis of strong-motion earthquake response spectra", Proceedings of U.S.-Japan Seminar on Earthquake Engineering Research with Emphasis on Lifeline Systems, Tokyo (1976).

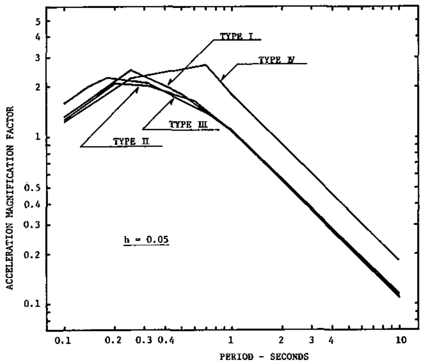

Fig.1. Example of Design Acceleration Magnification Spectra for Different Ground Conditions (see Table 1 for site classifications)

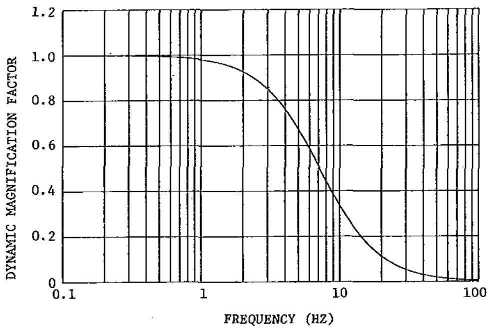

Fig.2. Frequency Characteristics of SMAC-B2 Accelerograph

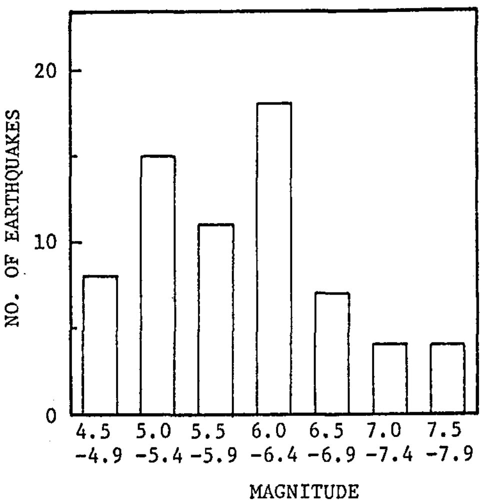

Fig.3. Histogram of Magnitudes of 67 Earthquakes Used for Analysis

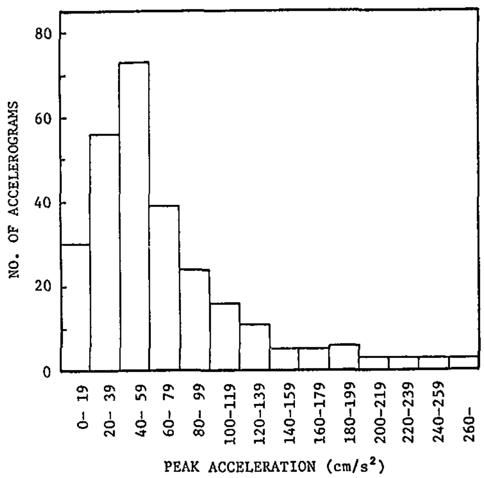

Fig.4. Histogram of Peak Accelerations of 277 Accelrograms Used for Analysis

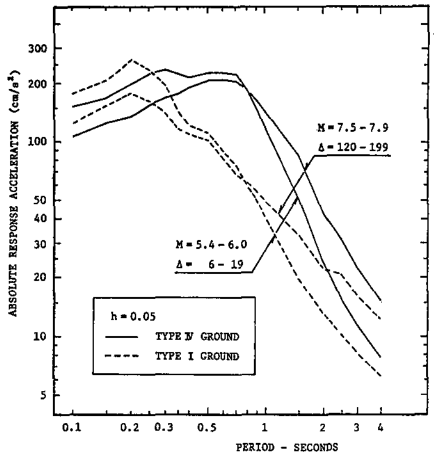

Fig.5. Examples of Predicted Acceleration Spectra

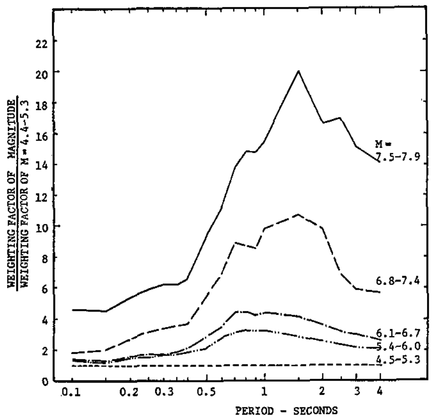

Fig.6. Effect of Magnitude on Acceleration Spectra

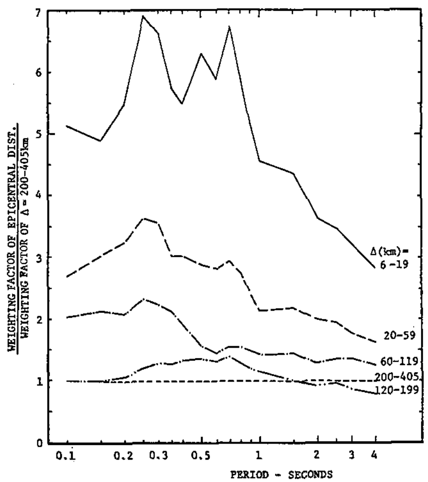

Fig.7. Effect of Epicentral Distance on Acceleration Spectra

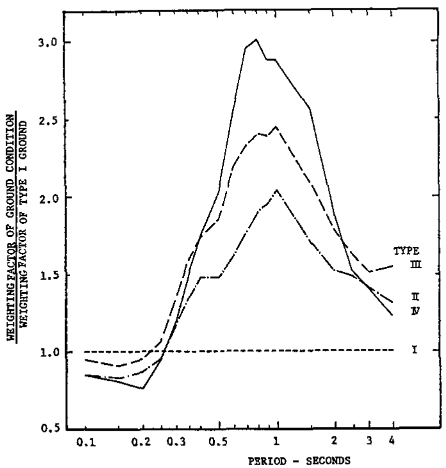

Fig.8. Effect of Ground Condition on Acceleration Spectra

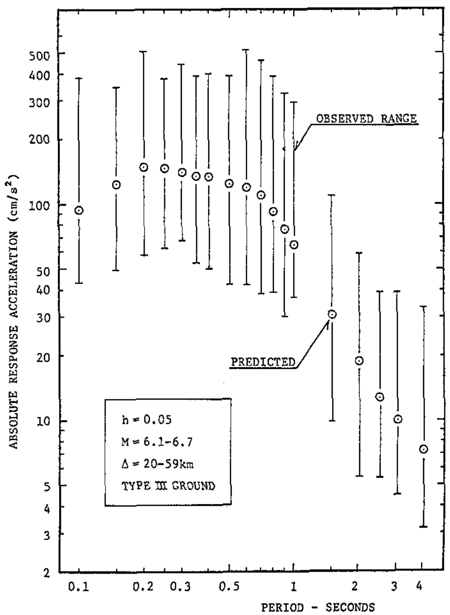

Fig.9. An Example of Observed Range and Predicted Value of Acceleration Spectral Amplitude

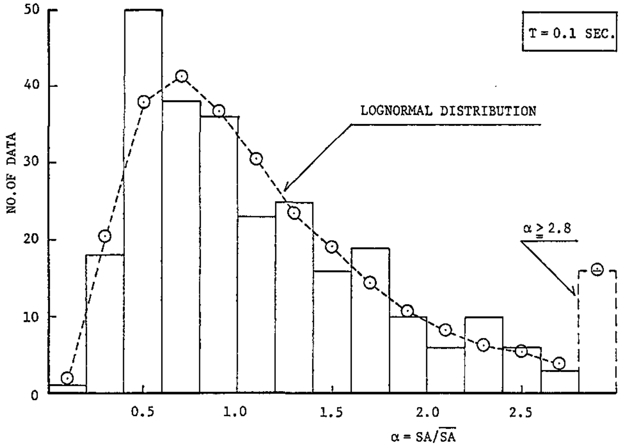

Fig.10. Histogram of α = SA/$\overline{SA}$
for T = 0.1 sec

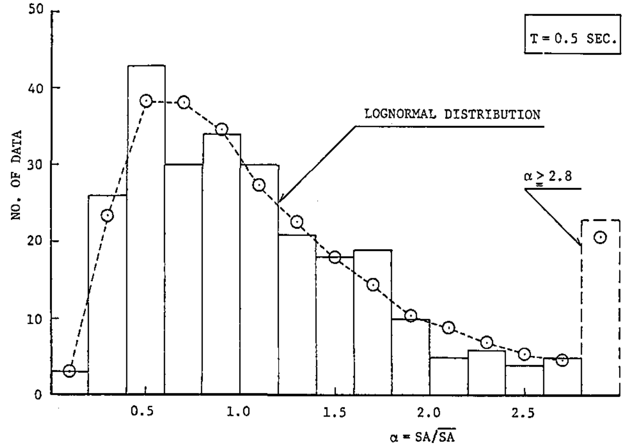

Fig.11. Histogram of α = SA/$\overline{SA}$
for T = 0.5 sec.

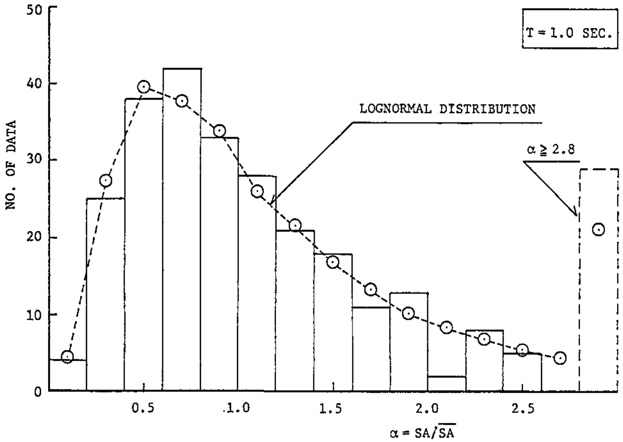

Fig.12. Histogram of α = SA/$\overline{SA}$
for T = 1.0 sec.

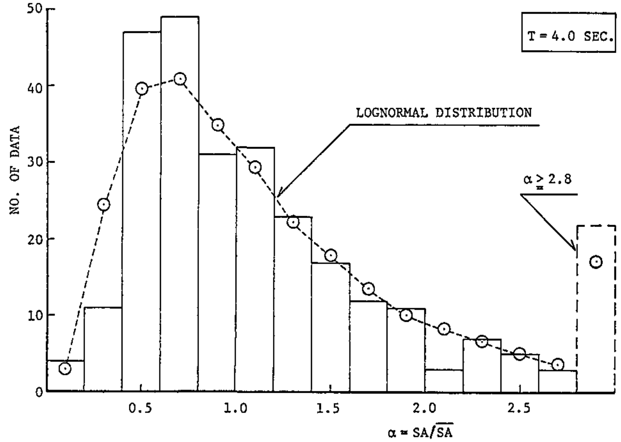

Fig.13. Histogram of α = SA/$\overline{SA}$
for T = 4.0 sec.

Table 1. Items and Categories Used for Quantification Analysis

ITEM	CATEGORY	MEAN FOR THE DATA IN EACH CATEGORY
EARTHQUAKE MAGNITUDE (M)	M = 4.5 ∼ 5.3	4.96
	M = 5.4 ∼ 6.0	5.75
	M = 6.1 ∼ 6.7	6.30
	M = 6.8 ∼ 7.4	7.06
	M = 7.5 ∼ 7.9	7.65
EPICENTRAL DISTANCE (Δ: km)	Δ = 6 ∼ 19	11.7
	Δ = 20 ∼ 59	38.2
	Δ = 60 ∼ 119	82.9
	Δ = 120 ∼ 199	158.7
	Δ = 200 ∼ 405	271.3
GROUND CONDITION AT RECORDING SITE	TYPE I : TERTIARY OR OLDER ROCK (DEFINED AS BEDROCK), OR DILUVIUM WITH H* < 10 m.	
	TYPE II: DILUVIUM WITH H ≧ 10 m, OR ALLUVIUM WITH H < 10 m.	
	TYPE III: ALLUVIUM WITH H < 25 m INCLUDING SOFT LAYER** WITH THICKNESS LESS THAN 5 m.	
	TYPE IV: OTHER THAN THE ABOVE, USUALLY SOFT ALLUVIUM OR RECLAIMED LAND.	

* DEPTH TO BEDROCK.

** SAND LAYER VULNERABLE TO LIQUEFACTION OR EXTREMELY SOFT COHESIVE SOIL LAYER.

Table 2. Distribution of Data Set

MAGNITUDE M	GROUND CONDITION	EPICENTRAL DISTANCE Δ (km)					TOTAL	
		6 ∿ 19	20 ∿ 59	60∿119	120∿199	200∿405		
4.5 ∿ 5.3	TYPE I	6	4				10	60
	TYPE II	4	10				14	
	TYPE III	12	8	8	2		30	
	TYPE IV	6					6	
5.4 ∿ 6.0	TYPE I		4	2			6	48
	TYPE II	4	4	4			12	
	TYPE III	2	12	6			20	
	TYPE IV	4	2	4			10	
6.1 ∿ 6.7	TYPE I		4	6			10	102
	TYPE II		4	4	2		10	
	TYPE III	4	32	22	8	2	68	
	TYPE IV		6	4	2	2	14	
6.8 ∿ 7.4	TYPE I			4	3	2	9	29
	TYPE II			2	4	2	8	
	TYPE III				4	4	8	
	TYPE IV					4	4	
7.5 ∿ 7.9	TYPE I				2	2	4	38
	TYPE II				6	2	8	
	TYPE III		2	6	4	2	14	
	TYPE IV				2	10	12	
TOTAL		42	92	72	39	32	277	

Table 3. Weighting Factors Obtained from Quantification Analysis

T*	ρ**	$f_M(T, 0.05)$ MAGNITUDE (M)					$f_\Delta(T, 0.05)$ EPICENTRAL DISTANCE (Δ: km)					$f_{GC}(T, 0.05)$ GROUND CONDITION (GC)			
		4.5∼5.3	5.4∼6.0	6.1∼6.7	6.8∼7.4	7.5∼7.9	6 ∼19	20∼59	60∼119	120∼199	200∼405	TYPE I	TYPE II	TYPE III	TYPE IV
0.10	0.56	0.218	0.278	0.296	0.399	1.00	5.10	2.67	2.05	0.994	1.00	126	107	120	106
0.15	0.53	0.225	0.274	0.297	0.448	1.00	4.85	3.01	2.15	1.00	1.00	155	130	141	125
0.20	0.54	0.185	0.280	0.288	0.499	1.00	5.48	3.24	2.07	1.05	1.00	169	149	161	129
0.25	0.55	0.171	0.254	0.283	0.534	1.00	6.86	3.65	2.33	1.21	1.00	135	129	143	129
0.30	0.56	0.164	0.269	0.280	0.548	1.00	6.59	3.51	2.25	1.27	1.00	109	130	147	131
0.35	0.55	0.161	0.274	0.302	0.588	1.00	5.74	3.05	2.13	1.24	1.00	92.8	126	149	142
0.40	0.57	0.152	0.268	0.311	0.557	1.00	5.45	3.01	1.92	1.33	1.00	83.0	122	145	144
0.50	0.63	0.108	0.237	0.309	0.593	1.00	6.35	2.91	1.60	1.36	1.00	76.6	113	140	156
0.60	0.67	0.0889	0.246	0.321	0.618	1.00	5.88	2.79	1.46	1.32	1.00	62.1	101	134	159
0.70	0.70	0.0730	0.222	0.315	0.644	1.00	6.77	2.96	1.56	1.37	1.00	50.0	88.8	118	148
0.80	0.68	0.0683	0.214	0.294	0.595	1.00	5.89	2.73	1.54	1.28	1.00	47.9	91.0	115	145
0.90	0.67	0.0672	0.214	0.285	0.581	1.00	5.13	2.38	1.48	1.20	1.00	46.4	90.5	113	136
1.00	0.67	0.0653	0.204	0.284	0.636	1.00	4.62	2.15	1.40	1.16	1.00	43.3	89.3	107	125
1.50	0.72	0.0503	0.138	0.204	0.534	1.00	4.40	2.20	1.44	1.00	1.00	33.0	56.5	68.5	84.6
2.00	0.71	0.0605	0.148	0.215	0.585	1.00	3.66	1.99	1.29	0.924	1.00	24.7	36.8	44.1	46.2
2.50	0.70	0.0587	0.136	0.183	0.405	1.00	3.50	1.95	1.34	0.947	1.00	21.9	32.7	35.8	33.0
3.00	0.69	0.0660	0.138	0.194	0.391	1.00	3.26	1.79	1.35	0.867	1.00	18.8	26.6	28.5	26.6
4.00	0.68	0.0704	0.144	0.187	0.395	1.00	2.81	1.61	1.27	0.788	1.00	15.7	20.3	24.1	19.1

*T = PERIOD (SECONDS), **ρ = CORRELATION COEFFICIENT

Table 4. Value of $\alpha = SA/\overline{SA}$ for Specified Probabilities of Being Exceeded

(1)	(2)	(3)	(4)	(5)					
T	m_α	σ_α	χ^2	VALUE OF α CORRESPONDING TO p.					
				p=0.05	p=0.1	p=0.2	p=0.3	p=0.4	p=0.5
0.1	1.24	0.910	11.78	2.94	2.32	1.75	1.41	1.18	1.00
0.15	1.25	0.882	31.66	2.90	2.31	1.74	1.42	1.20	1.02
0.2	1.27	0.914	26.34	2.98	2.36	1.77	1.44	1.21	1.03
0.25	1.26	0.968	19.78	3.06	2.39	1.77	1.43	1.19	1.00
0.3	1.26	0.948	10.19	3.04	2.38	1.78	1.43	1.20	1.01
0.35	1.29	1.10	9.01	3.31	2.53	1.83	1.45	1.18	0.98
0.4	1.26	0.999	11.50	3.12	2.42	1.78	1.42	1.18	0.99
0.5	1.30	1.05	6.93	3.24	2.51	1.84	1.46	1.21	1.01
0.6	1.29	1.11	10.40	3.33	2.54	1.83	1.44	1.18	0.98
0.7	1.34	1.32	16.80	3.70	2.74	1.91	1.47	1.18	0.96
0.8*	1.27	1.02	9.56	3.16	2.45	1.79	1.43	1.18	0.99
0.9*	1.29	1.08	12.55	3.28	2.52	1.83	1.45	1.19	0.99
1.0*	1.28	1.09	14.47	3.28	2.51	1.81	1.43	1.17	0.97
1.5*	1.23	1.00	17.01	3.08	2.38	1.74	1.39	1.14	0.95
2.0*	1.23	0.956	7.37	3.01	2.35	1.73	1.39	1.16	0.97
2.5*	1.27	1.14	14.97	3.34	2.53	1.80	1.41	1.15	0.95
3.0*	1.24	1.01	19.45	3.11	2.40	1.75	1.40	1.15	0.96
4.0*	1.23	0.953	16.49	3.00	2.34	1.73	1.39	1.16	0.97
AVERAGE				3.16	2.44	1.79	1.43	1.18	0.99

(1) T = PERIOD (SECONDS)

(2) m_α = MEAN OF α

(3) σ_α = STANDARD DEVIATION OF α

(4) $\chi^2 = \sum_{i=1}^{15} \frac{(F_i - f_i)^2}{F_i}$ $\qquad \chi^2_{0.05,12} = 21.03$

F_i = EXPECTED NO. OF OCCURRENCES

f_i = OBSERVED NO. OF OCCURRENCES

(5) p = PROBABILITY OF BEING EXCEEDED

* TWO DATA OMITTED FOR CALCULATION OF m_α, σ_α.